Assessment of imaging with extended depth-of-field by means of the light sword lens in terms of visual acuity scale

Karol Kakarenko,[1] Izabela Ducin,[1] Krzysztof Grabowiecki,[2] Zbigniew Jaroszewicz,[1,3] Andrzej Kolodziejczyk,[1] Alejandro Mira-Agudelo,[4] Krzysztof Petelczyc,[1,*] Aleksandra Składowska,[1,5] and Maciej Sypek[6]

[1]*Faculty of Physics, Warsaw University of Technology Koszykowa 75, 00-662 Warsaw, Poland*
[2]*CIM-mes Projekt sp. z o.o., Al. Jerozolimskie 125/127 loc. 503, 02-017 Warsaw, Poland*
[3]*Institute of Applied Optics, Kamionkowska 18, 03-805 Warsaw, Poland*
[4]*Grupo de Óptica y Fotónica, Instituto de Física, Facultad de Ciencias Exactas y Naturales, Universidad de Antioquia UdeA, Calle 70 No. 52-21, Medellín, Colombia*
[5]*Laboratory of Visual System, Department of Neurophysiology, Nencki Institute of Experimental Biology, Pasteura 3, 02-093 Warsaw, Poland*
[6]*SKA Polska sp. z o.o., Al. Jerozolimskie 125/127 room 406, 02-017 Warsaw, Poland*
[*] *krzys137@if.pw.edu.pl*

Abstract: We present outcomes of an imaging experiment using the refractive light sword lens (LSL) as a contact lens in an optical system that serves as a simplified model of the presbyopic eye. The results show that the LSL produces significant improvements in visual acuity of the simplified presbyopic eye model over a wide range of defocus. Therefore, this element can be an interesting alternative for the multifocal contact and intraocular lenses currently used in ophthalmology. The second part of the article discusses possible modifications of the LSL profile in order to render it more suitable for fabrication and ophthalmological applications.

References and links

1. J. A. Davison and M. J. Simpson, "History and development of the apodized diffractive intraocular lens," J. Cataract Refract. Surg. **32**(5), 849–858 (2006).
2. B. Żelichowska, M. Rękas, A. Stankiewicz, A. Cerviño, and R. Montés-Micó, "Apodized diffractive versus refractive multifocal intraocular lenses: Optical and visual evaluation," J. Cataract Refract. Surg. **34**(12), 2036–2042 (2008).
3. A. Zlotnik, S. Ben Yaish, O. Yehezkel, K. Lahav-Yacouel, M. Belkin, and Z. Zalevsky, "Extended depth of focus contact lenses for presbyopia," Opt. Lett. **34**(14), 2219–2221 (2009).
4. S. Zheng, Z. Wang, Y. Liu, and R. Li, "Aspheric spectacles for correcting presbyopia with myopia and astigmatism," Appl. Opt. **51**(29), 6926–6932 (2012).
5. T. Zhao, A. Liu, Q. Liu, and F. Yu, "Axial intensity distribution analysis for a depth-of-field-extended optical system using a low-frequency binary phase mask," Appl. Opt. **53**(17), 3782–3786 (2014).
6. J. H. McLeod, "The Axicon: A New Type of Optical Element," J. Opt. Soc. Am. **44**(8), 592 (1954).
7. J. Sochacki, A. Kołodziejczyk, Z. Jaroszewicz, and S. Bará, "Nonparaxial design of generalized axicons," Appl. Opt. **31**(25), 5326–5330 (1992).
8. W. Chi and N. George, "Electronic imaging using a logarithmic asphere," Opt. Lett. **26**(12), 875–877 (2001).
9. J. Ares, R. Flores, S. Bará, and Z. Jaroszewicz, "Presbyopia compensation with a quartic axicon," Optom. Vis. Sci. **82**(12), 1071–1078 (2005).
10. E. A. Villegas, E. Alcón, S. Mirabet, I. Yago, J. M. Marín, and P. Artal, "Extended depth of focus with induced spherical aberration in light-adjustable intraocular lenses," Am. J. Ophthalmol. **157**(1), 142–149 (2014).
11. A. Kołodziejczyk, S. Bará, Z. Jaroszewicz, and M. Sypek, "The light sword optical element - a new diffraction structure with extended depth of focus," J. Mod. Opt. **37**(8), 1283–1286 (1990).
12. G. Mikuła, Z. Jaroszewicz, A. Kolodziejczyk, K. Petelczyc, and M. Sypek, "Imaging with extended focal depth by means of lenses with radial and angular modulation," Opt. Express **15**(15), 9184–9193 (2007).

13. J. Ares García, S. Bará, M. Gomez García, Z. Jaroszewicz, A. Kolodziejczyk, and K. Petelczyc, "Imaging with extended focal depth by means of the refractive light sword optical element," Opt. Express **16**(22), 18371–18378 (2008).
14. K. Petelczyc, J. Ares Garcia, S. Bará, Z. Jaroszewicz, A. Kolodziejczyk, and M. Sypek, "Presbyopia compensation with a light sword optical element of a variable diameter," Photon. Lett. Poland **1**, 55–57 (2009).
15. K. Petelczyc, J. A. García, S. Bará, Z. Jaroszewicz, K. Kakarenko, A. Kolodziejczyk, and M. Sypek, "Strehl ratios characterizing optical elements designed for presbyopia compensation," Opt. Express **19**(9), 8693–8699 (2011).
16. A. A. Gallego, S. Bará, Z. Jaroszewicz, and A. Kolodziejczyk, "Visual Strehl performance of IOL designs with extended depth of focus," Optom. Vis. Sci. **89**(12), 1702–1707 (2012).
17. K. Petelczyc, S. Bará, A. Ciro López, Z. Jaroszewicz, K. Kakarenko, A. Kolodziejczyk, and M. Sypek, "Contrast transfer properties of the light sword optical element designed for presbyopia compensation," J. Eur. Opt. Soc. Rapid Publ. **6**, 11053 (2011).
18. K. Petelczyc, S. Bará, A. C. Lopez, Z. Jaroszewicz, K. Kakarenko, A. Kolodziejczyk, and M. Sypek, "Imaging properties of the light sword optical element used as a contact lens in a presbyopic eye model," Opt. Express **19**(25), 25602–25616 (2011).
19. J. A. Venter, M. Pelouskova, C. E. Bull, S. C. Schallhorn, and S. J. Hannan, "Visual outcomes and patient satisfaction with a rotational asymmetric refractive intraocular lens for emmetropic presbyopia," J. Cataract Refract. Surg. **41**(3), 585–593 (2015).
20. K. Grabowiecki, "LIGHTSWORDS lens promises to reduce age-related degradation of sight," http://cordis.europa.eu/news/rcn/122565_en.html, accessed 4/1/15.
21. A. Valberg, *Light Vision Color* (John Wiley & Sons, 2005).
22. H. Gross, F. Blechinger, and B. Achtner, *Handbook of Optical Systems*, Vol. 4, Survey of Optical Instruments (Wiley-VCH, 2008).
23. D. R. Williams, "Topography of the foveal cone mosaic in the living human eye," Vision Res. **28**(3), 433–454 (1988).
24. J. T. Holladay and Msee, "Visual acuity measurements," J. Cataract Refract. Surg. **30**(2), 287–290 (2004).
25. I. L. Bailey and J. E. Lovie, "New design principles for visual acuity letter charts," Am. J. Optom. Physiol. Opt. **53**(11), 740–745 (1976).
26. A. Colenbrander, "Visual standards: Aspects and ranges of vision loss" Report prepared for the 29th International Congress of the International Council of Ophthalmology, Sydney, Australia, 2002.
27. Z. Zalevsky, S. Ben Yaish, A. Zlotnik, O. Yehezkel, and M. Belkin, "Cortical adaptation and visual enhancement," Opt. Lett. **35**(18), 3066–3068 (2010).
28. P. Artal, L. Chen, E. J. Fernández, B. Singer, S. Manzanera, and D. R. Williams, "Neural compensation for the eye's optical aberrations," J. Vis. **4**(4), 281–287 (2004).
29. J. T. Holladay, M. J. Lynn, G. O. Waring 3rd, M. Gemmill, G. C. Keehn, and B. Fielding, "The Relationship of Visual Acuity, Refractive Error, and Pupil Size After Radial Keratotomy," Arch. Ophthalmol. **109**(1), 70–76 (1991).
30. J. A. Jordan, Jr., P. M. Hirsch, L. B. Lesem, and D. L. Van Rooy, "Kinoform Lenses," Appl. Opt. **9**(8), 1883–1887 (1970).
31. M. Sypek, "Light propagation in the Fresnel region. New numerical approach," Opt. Commun. **116**(1–3), 43–48 (1995).
32. M. Sypek, C. Prokopowicz, and M. Gorecki, "Image multiplying and high-frequency oscillations effects in the Fresnel region light propagation simulation," Opt. Eng. **42**(11), 3158–3164 (2003).

1. Introduction

Insufficient accommodation range, as it occurs in the case of presbyopia, is a frequent and difficult problem that affects the sight of many people. Various proposals of ophthalmic lenses aimed to compensate for this deficiency have been investigated. In general, they can be divided into three main families: accommodative proposals, multifocal proposals, and proposals with Extended Depth of Field (EDF). Between the members of the second group, there can be found bifocal or multifocal lenses [1,2], whereas in the last group one can find rotationally symmetric phase masks [3–5], axicons [6–8], lenses with negative spherical aberration [9,10], and light sword optical elements (LSOEs) [11–13]. In contrast to other elements, the LSOEs are distinguished by angular variation of the optical power. This gives rise to one of their important advantages as compared with the remaining elements: namely, the independence of their optical power range with respect to the pupil's diameter [14]. Numerical simulations and experiments have demonstrated interesting characteristics of the LSOEs in terms of their uniformity, high Strehl ratios [15], and the visual Strehl ratio [16] within the assumed range of defocus. Their imaging properties have also been analyzed by means of the modulation transfer function (MTF) [17] and through the calculation of two

parameters showing similarity between the object and its image: namely, a root mean square deviation and a correlation coefficient [18].

Similarly to the MPlus lens by Oculentis, recently available in the market [19], the LSOE is not rotationally symmetric. The MPlus lens has only two angular sectors with different optical powers and a small transition zone, while in the case of the LSOE every infinitesimal angular sector has its own focal length. In order to avoid unwanted chromatic aberrations in the ophthalmic applications refractive version of the LSOE (hereafter referred to as the light sword lens (LSL)) is necessary. However, the LSL reveals a complicated profile. The surface curvature of such an element continuously and smoothly varies across the entire surface, which results in the discontinuity observed as a radially placed edge or step (see Fig. 1 below). When this manufacturing issue is considered, the technologies have to be exploited, where demand for micrometer accuracy has to be combined with smooth, continuous surface conditions and sharp edge manufacturability. Therefore, fabrication of the LSL represents serious problems and demands. As a result, up to now only two promising, qualitative experiments with LSLs have been presented [13, 18]. Such refractive elements were fabricated by the non-uniform exposure of photoresist, but they nevertheless demonstrated distinct aberrations. In order to produce the LSL with parameters for presbyopia correction, a wide cooperation project was launched resulting in the fabrication of LSLs with acceptable quality [20]. The obtained method relies on precise micromachining and molding injection technology .

In response to these considerations, we have decided to investigate the LSL in terms of the simulated attainable visual acuity (VA) for the range of optical powers varying from 0 diopter (when the object is located at infinity) to 4 diopters (corresponding to the near vision object plane situated at 25 cm). It is necessary to note that our intention was not an accurate modeling of the human eye and human vision. We used a simple optical setup inspired by the eye optical system in order to investigate EDF properties in terms of optometric criteria. Therefore presented results should be regarded as relative ones suggesting potential usefulness of the LSL for presbyopia compensation only.
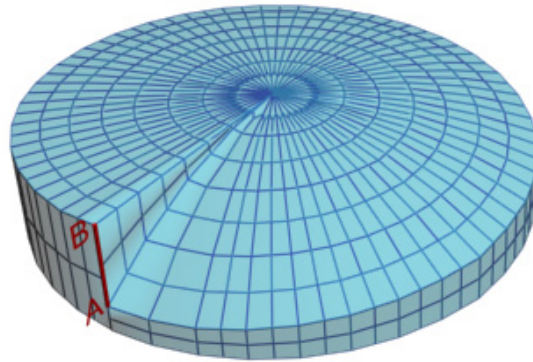

Fig. 1. Shape of the light sword lens (LSL) element.

2. The simplified presbyopic eye and the LSL element

In order to assess the characteristics of VA, we used the imaging optical setup (termed the simplified presbyopic eye) inspired by the schematic Gullstrand-Emsley parameterization [21, 22] (hereafter referred to as the Gullstrand eye) and presented in our earlier publication [18]. The main assumption of our design was to preserve an image size and depth of field properties of the Gullstrand eye when we replace aqueous and vitreous humors (n = 1.336) with air (n = 1.000). This modification substantially simplifies the practical realization of the model, but it causes some changes in its parameters. In order to achieve the same size of

output image, unalterable interior focal lengths should be accompanied with the proper rescaling of experimental parameters. We consequently reduced the optical power of the lenses referred to the cornea and crystalline lens by a factor of 1.336. Owing to the lower optical power and the symmetry of corneal focal lengths (unlike that of the Gullstrand eye), we imposed an increase in the objects distances by the same factor. It is compensated by higher magnification of the optical system resulting in the same size and resolution of an image compared with the Gullstrand eye. A test chart, which the Gullstrand eye should recognize from some distance, must be placed 1.336 times farther. Unlike the setup presented in [18] we used a 3 mm diaphragm (referring to optimal lighting conditions in photopic vision) placed just before the second lens (i.e., the modeling crystalline lens of the Gullstrand eye), therefore rescaling of the pupil diameter was not necessary. We modeled the retina with a 1/3′ CCD array (Sony ICX445 AL/AQ) with 3.75 μm x 3.75 μm pixel size [23]

The simplified presbyopic eye is an idealized model of the human eye which simulates only some aspects of the image formed on the retina. For instance, it does not reproduce the monochromatic or chromatic aberrations of the real eye. The experimental results can therefore be interpreted only in terms of relative effects of the LSL on the depth of field.

The LSL used to add the EDF feature is described by the following shape function, defining the thickness of the element [17]:

$$\Delta l\left(r,\theta\right) = l_{max} - \frac{\Delta D \theta r^2}{4\pi\left(n-1\right)}, \tag{1}$$

where n denotes the refractive index, l_{max} denotes the maximal thickness of the element, and $\Delta D = 3$ diopters denotes the maximal addition of optical power made by the element (according to the functional vision range). θ and r are the angular and radial coordinates, respectively. This means that the thickness of the LSL depends not only on the radial coordinate but also on the angular coordinate.

The refractive form of the LSL designed according to Eq. (1) and illustrated in Fig. 1 was fabricated using the recently obtained breakthrough technology based on micromachining. To manufacture the required shape of the LSL in small groups of samples necessary for research, we selected the molding injection technology (Fig. 2). The sample material was polymethylmethacrylate (PMMA). The mold developed with an advanced method was characterized by the cavity surface roughness being kept within 20 nm, and the shape tolerances not exceeding 2 μm. To validate the proposed method, we verified the geometry with the use of the profilometer Veeco Wyko NT9300 (USA) (Fig. 3). The optical characterization was performed with the classical Mach-Zender interferometer assembled in our optical laboratory (Fig. 4). The following dimensional constraints of fabricated LSLs were achieved: maximum surface roughness: 150 nm; average surface roughness: 37 nm; maximum local deviation from the ideal profile: ± 500 nm; step edge definition: (angle to normal direction) 0–30°.

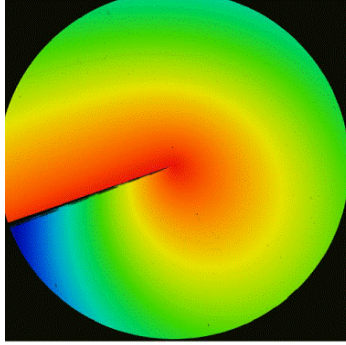Fig. 2. Samples of polymethylmethacrylate light sword lenses (LSLs) fabricated by injection technology.

Fig. 3. Profile of the light sword lens (LSL) sample used, measured by the profilometer Veeco Wyko NT9300 with a linear color scale (blue = 0 μm; red = 50 μm).
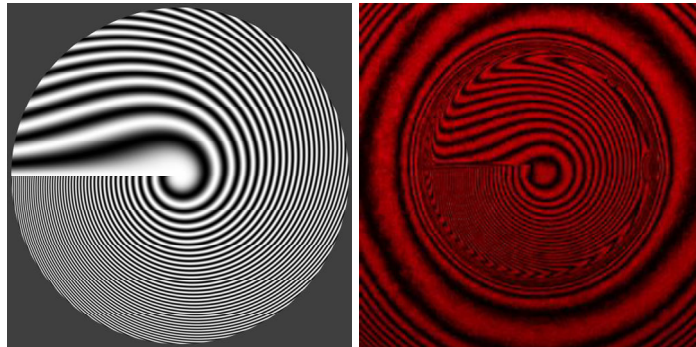

Fig. 4. The numerical interferogram of the ideal light sword lens (LSL) (left) and the interferogram of the LSL sample used, obtained with a Mach-Zehnder interferometer using monochromatic light with λ = 632.8 nm.

3. Assessment of VA of the simplified eye model with Early Treatment Diabetic Retinopathy Study (ETDRS) charts

Deficiencies of traditional Snellen charts have been frequently raised [24], and in response LogMAR (logarithm of the minimum angle of resolution) test cards based on geometric progression have been investigated [25]. Our optical setup to assess VA of the simplified eye model, based on the ETDRS standard [26], is shown in Fig. 5. Test charts had 14 lines corresponding to LogMAR values from −0.3 to 1.0 (in the Snellen scale, VA values from 0.1 to 2.0). The tests were performed in photopic conditions with white light of about 200 cd/m^2 and with sufficiently large contrast values [26]. We choose different charts for each distance, equal to the defocus of the Gullstrand eye from 4 diopters to 0 diopter, with a step of 0.5 diopter (corresponding sight distances: 250 mm, 286 mm, 333 mm, 400 mm, 500 mm, 667 mm, 100 cm, 200 cm, and 500 cm, the last of which is assumed as being equivalent to infinity). In the experiment, we used distances rescaled by a factor of 1.336 in order to compensate for the lower optical power of our simplified presbyopic eye focused on infinity and its higher optical magnification. Therefore we maintained the unchanged angular appearance of the eyechart letters.
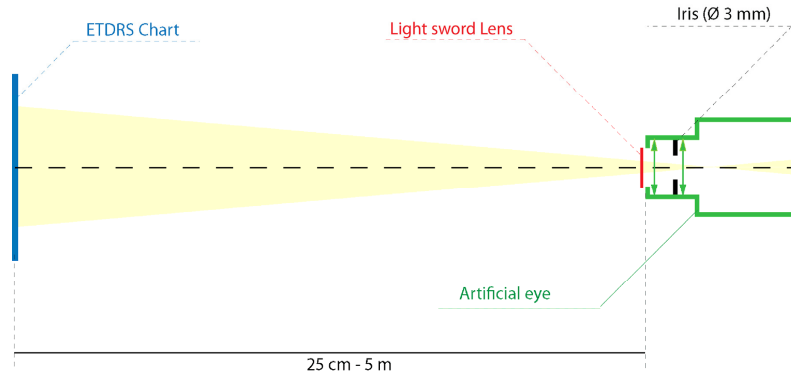
Fig. 5. Optical arrangement for imaging using the simplified presbyopic eye and the light sword lens (LSL) element.

We recorded images of test charts formed by the simplified presbyopic eye described above, and also with the LSL element playing the role of contact lens in the front of the lens system (Fig. 6). The obtained images were interpreted on the computer screen (with zooming ability) by a group of 10 young (i.e., 25–35 years old) observers. Recognitions were scored in a LogMAR scale based on a line-by-line method [26], and were then transformed into the Snellen scale (VA) as:

$$VA = 10^{-\log MAR}. \tag{2}$$

4. Results

Figure 6 shows the experimentally recorded color images of the ETDRS test charts. One can observe a satisfactory extension of the depth of field, accompanied by a slight decrease of contrast – especially for distant and near charts. Chromatic aberrations are almost not visible. On the other hand, one must take into account the fact that our model does not consider aberrations of the real human eye. Figure 7 presents a movie with numerical simulations of the same experiment in monochromatic light (λ = 555 nm) with shots made every 0.05 D, which allows for continuous observation of the varying sharpness of the images formed by the simplified presbyopic eye with and without the superposed LSL element. All given object distances and defocusing values were rescaled to the Gullstrand eye.

It can be noted in Fig. 7 that, because of the partly off-axis character of the LSL imaging capability, a small waving of the image takes place with displacements of less than 3 arcmin (0.087 prism diopter). It is a natural consequence of the lack of rotational symmetry in the LSL shape, which causes the focusing of light into the off-axis direction perpendicular to the actual focusing angular segment [12]. The ability of the human visual system to adapt to this situation remains to be investigated, with some studies indicating high flexibility [27, 28].

It may be concluded that VA assessed in the simplified presbyopic eye after correction by the LSL is at least 0.6. At the whole range of defocus (i.e., 0–4 D), results correspond to normal vision [26]. In the reference case for defocus values greater than −1 D, VA is below 0.3, which is the lower limit of vision with slight impairment [26]. The results shown in Fig. 6 can be collected into a single plot (Fig. 8), which shows more distinctly the performance of the LSL element in comparison with the simplified presbyopic eye.
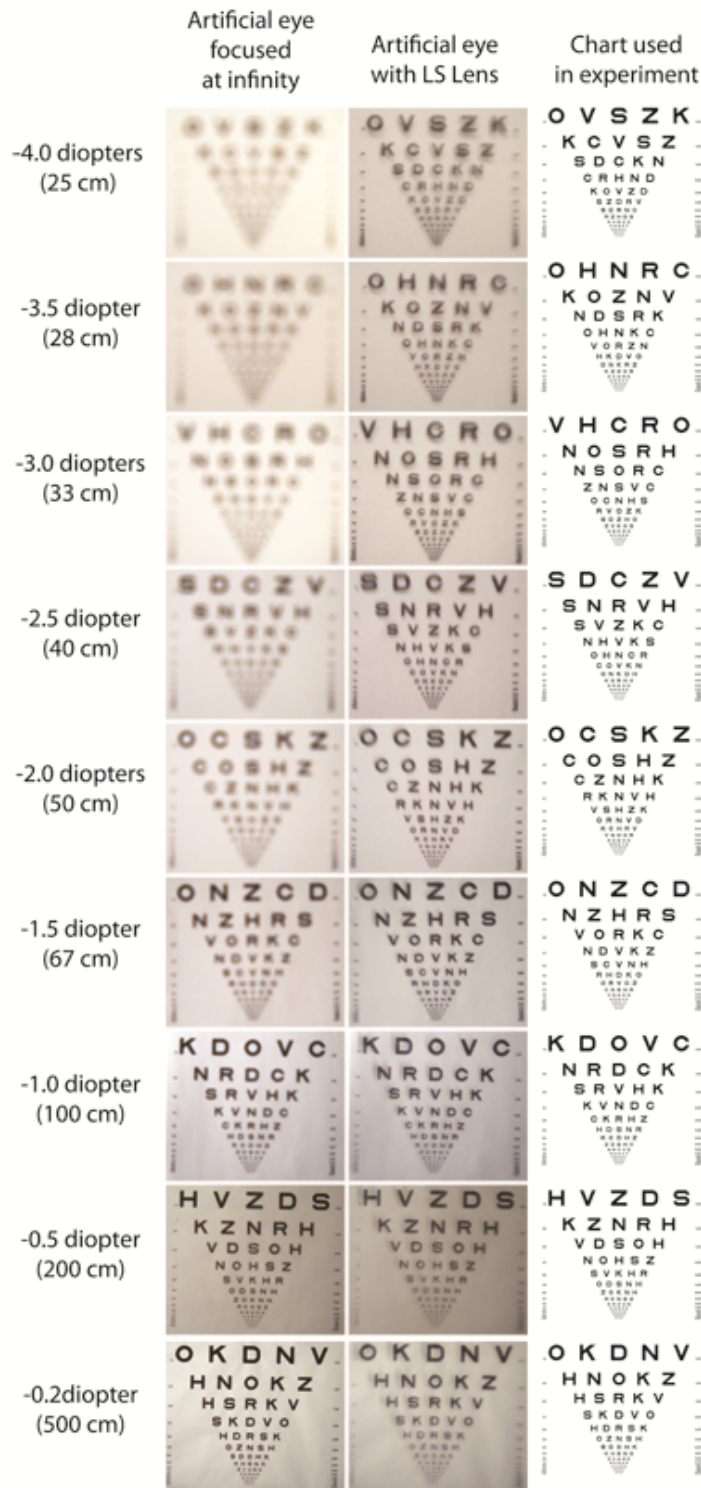
Fig. 6. Relative comparison of ETDRS charts imaged experimentally by the simplified presbyopic eye (iris diameter: 3 mm) without (left column) and with (middle column) the light sword lens (LSL). See Media 1 for high resolution.
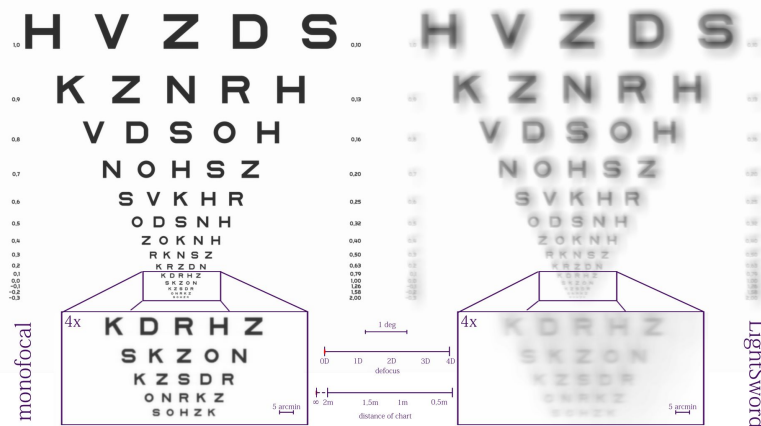
Fig. 7. High-resolution movie (Media 2) of relative comparison of the simulated ETDRS chart images formed by the simplified presbyopic eye alone (left image) and with the light sword lens (LSL) added (right image). Counters of the defocus values and related object distances rescaled to the Gullstrand eye are given in the center of the image.

To estimate the VA of the simplified presbyopic eye with and without LSL compensation, we chose a group of 10 volunteers. Their task was to recognize the optotypes of the ETDRS charts imaged by the simplified presbyopic eye (Fig. 6). Images were displayed on a LCD screen and could be zoomed if necessary. According to line-by-line scoring [26], the result of the VA was connected with the last line in which the observer was able to recognize more than half of the signs, taking into account signs recognized in the next line. The VA of the simplified presbyopic eye was adopted to be the mean of the observer recognition results for every distance. The uncertainty of the VA is the standard deviation, and the maximal error of the position of the charts is assumed to be 1 cm.
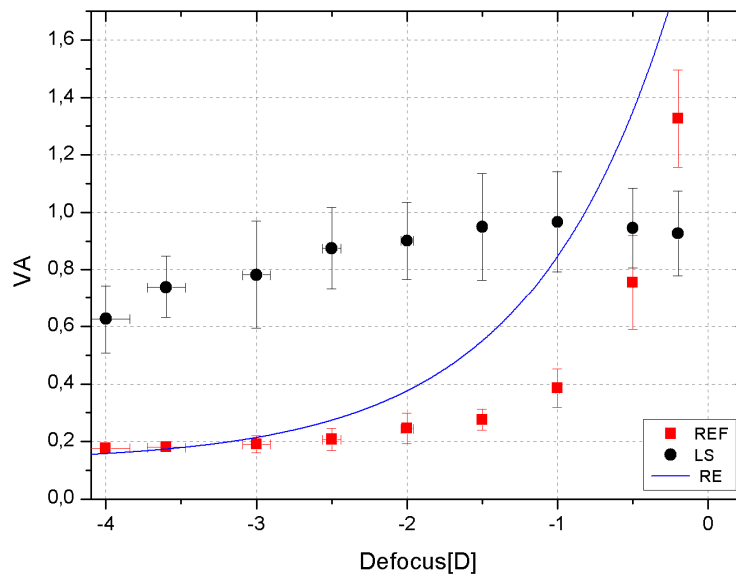

Fig. 8. Assessment of visual acuity (VA) of the simplified presbyopic eye for different values of defocus, rescaled to the Gullstrand eye. Red marks correspond to tests without the light sword lens (LSL). Black marks correspond to tests with the LSL. The blue line corresponds to the real normal eye with 3 mm diameter pupil (based on [29]).

In our opinion, Fig. 8 represents the most convincing proof of the LSL imaging capacity with extended depth of field. Nevertheless one should take into account the relative nature of the results. The results show the effect of the LSL on the depth of field in our simplified eye model. Our simplified presbyopic eye does not consider monochromatic and chromatic aberrations of the real human eye, nor the neurophysiology of vision. Therefore, the measured VA does not represent exactly the visual acuity that would be obtained in a real eye.

5. Problem of the LSL's shape discontinuity

A serious drawback of the LSL seems to be the discontinuity of its shape that results from the direct neighborhood of sectors given by $\theta = 0$ ($\Delta l = l_{max}$) and by $\theta = 2\pi$ ($\Delta l = l_{max}-\Delta DR^2/2(n-1)$), where R is a semidiameter of the element. Therefore, the profile of the refractive element visible in Fig. 1 manifests the sharp edge AB of height $\Delta DR^2/2(n-1)$, corresponding in our case to a value of about 48 μm ($\Delta D = 3$ D, $R = 4$ mm, and $n \approx 1.5$).
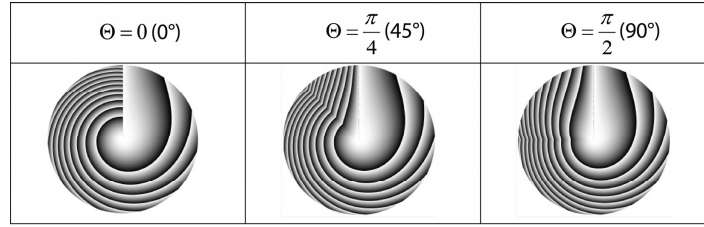

Fig. 9. The light sword lens (LSL) with phase discontinuity ($\Theta = 0$), and modified LSLs without phase discontinuity. Angular sectors of oppositely growing dioptric power with widths $\Theta = \pi/4$ and $\pi/2$, respectively, were implemented in the second and third cases. Elements are presented in the form of a kinoform [30].

Note that this value must grow by a scaling factor if the LSL is applied as an intraocular lens because of the higher refractive index of the surrounding media. Such a sharp step may be the reason for at least three important inconveniences. The first inconvenience is of a technological nature: LSLs are easier to fabricate when such shape discontinuities are not present. Second, a sharp step of this dimension can irritate the human eye, or possibly even damage some ocular tissue. Third, it can be a source of disturbing edge wave. However, the linear function of the angular coordinate θ given by Eq. (1) can be changed. By skillful manipulation of the dependence of the optical power on the angle θ, we can avoid the unwanted sharp edge without a noticeable degradation of output images. An example of one possible solution is given below with numerical simulations performed for monochromatic phase masks corresponding to the studied element.

In order to eliminate the needless discontinuity, we introduce into the LSL surface an angular sector of a width equal to Θ (see Fig. 9), where the thickness of the element changes linearly. According to Eq. (1), such a sector is equivalent to the LSL with the dioptric power increasing gradually from the value 0 to the value ΔD, oppositely to the rest of area occupied by the common LSL:

$$\Delta l(r,\theta;\Theta) = \begin{cases} l_{max} - \dfrac{\Delta D\theta r^2}{2(2\pi-\Theta)(n-1)} & for\ 0 < \theta \le 2\pi - \Theta \\[4mm] l_{max} - \dfrac{\Delta Dr^2(2\pi-\theta)}{2\Theta(n-1)} & for\ 2\pi - \Theta < \theta \le 2\pi \end{cases} \quad (3)$$

In this way, both junctions remain continuous (Fig. 9). We conducted numerical simulations of imaging for the elements shown in Fig. 9 based on the modified convolution method [31, 32]. The obtained results of imaging for object distances corresponding to the performed experiment are presented in Fig. 10. Numerical simulations were conducted for the simplified presbyopic eye used in the experiment. The objects used were Snellen optotypes

with angular dimensions 5 arcmin. corresponding to VA = 1.0. We assumed monochromatic, spatially incoherent light with a wavelength of 555 nm, corresponding to the highest sensitivity of the human eye in photopic vision [21, 22]. We also used phase masks as counterparts (kinoforms [30]) of refractive elements defined by Eq. (3). It can be seen that the quality of imaging, though it continuously deteriorates with the increasing angle of the discontinuity-removing sector, still offers a satisfactorily broad range of distances where the image remains comparable with that obtained with the conventional LSL. A modification area limited to the angle of 45° (or even less) allows us to avoid the unwanted sharp step of the LSL profile, and does not exhibit a noticeable influence on the quality of output images.
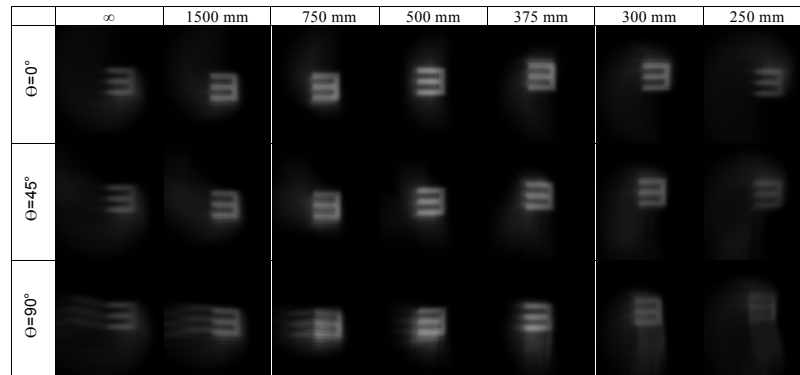

Fig. 10. Simulated output images formed by the light sword lens (LSL), as well as the modified LSL with discontinuities removed.

6. Conclusions

We have demonstrated EDF imaging realized by means of the LSL in the simplified presbyopic eye. According to previously reported theoretical studies, numerical simulations, and qualitative experiments [12–18], an element of this kind can form recognizable images of acceptable quality in the presence of a defocus of 0–4 diopters. The LSL demonstrated its superiority over other solutions designed especially for multifocal and EDF imaging. The LSL lacks rotational symmetry and exhibits a junction, rendering its fabrication extremely difficult, which requires a new and sophisticated method. The essential breakthrough has been offered by the lately elaborated technology based on precise micromachining and injection molding. It enabled us to produce non-symmetrical elements of a satisfactory quality. Therefore, we could realize a quantitative experiment illustrating the VA assessment of output images formed in the simplified presbyopic eye corrected by the LSL. According to the obtained results, the VA is at least 0.6 for the assumed defocusing, which reaches up to 4 diopters. Therefore, taking into account present standards, the LSL exhibits an interesting possibility to recover normal vision [25].

The main drawback of the refractive element is a sharp step in its profile (Fig. 1), which renders fabrication processes more difficult. Moreover, such an edge can be harmful for the human eye with the LSL applied as a contact lens or an intraocular lens. Therefore, in the final part of the paper we presented numerical simulations illustrating that this drawback can be avoided without noticeable influence on the quality of output images.

One should take into account the limitations of our approach – in particular, the use of a simple optical setup to model the eye. The eye model does not reproduce the aberrations of the real human eye or the effect of visual processing by the brain on visual acuity. Therefore the visual acuity produced by the setup is not expected to correspond precisely to the visual acuity of a real eye. Moreover, some important problems related to the LSL applied to the human eye lie outside the scope of this paper and require further detailed studies. It is necessary to briefly mention the tilt and decentration of the element, and the influence of the

LSL junction on vision comfort. According to [17], the MTFs illustrating imaging realized by the LSL have nonzero values for wide ranges of frequencies and do not exhibit substantial oscillations. On the other hand, for defocusing values close to 0 diopter, these MTFs have small values for a large range of spatial frequencies. Accordingly, perhaps this disadvantage will demand future correction of the LSL design.

The ultimate solution can be obtained after fabrication of LSLs in the form of contact or intraocular lenses, together with medical tests. However, taking into account the results presented here (and in former studies), the refractive LSLs with angular modulation of optical power seem to be a very attractive alternative to the contact and intraocular lenses presently available in the market.

Acknowledgments